

# **Contemporary of Sciences**

**Physics, Chemistry and Mathematics**

**Editor:  
DENNIS LING**

**Contributing Authors:  
ANITA RAMLI  
BEH HOE GUAN  
BALBIR SINGH MAHINDER SINGH  
CECILIA DEVI WILFRED  
CHONG FAI KAIT  
HAMZAH SAKIDIN  
HANITA DAUD  
HASNAH M Zaid  
HASSAN SOLEIMANI  
LEE KEAN CHUAN  
LIM JUN WEI  
RADZUAN RAZALI  
TANG TOON BOON**

**Volume 1**

Copyright © 2015

PUBLISHED BY UTP PRESS

ISBN: XX-XXXX-XX

Licensed under the UTP Press, Universiti Teknologi PETRONAS (the “License”). You may not use this file except in compliance with the License. You may obtain a copy of the License from UTP Press, Universiti Teknologi PETRONAS. Unless required by applicable law or agreed to in writing, software distributed under the License is distributed on an “AS IS” BASIS, WITHOUT WARRANTIES OR CONDITIONS OF ANY KIND, either express or implied. See the License for the specific language governing permissions and limitations under the License.

*First printing, November 2015*

# Contents

	Physics	
<b>1</b>	<b>Ferrite-CNT-Polymer Composite</b> .....	<b>11</b>
<b>1.1</b>	<b>Introduction</b>	<b>11</b>
<b>1.2</b>	<b>Experimental</b>	<b>13</b>
1.2.1	Materials .....	13
1.2.2	Ferrite pereparation .....	13
1.2.3	Composite preparation .....	13
1.2.4	Characterization .....	14
<b>1.3</b>	<b>Results and discussion</b>	<b>14</b>
1.3.1	Microstructural and morphological analysis .....	14
1.3.2	Magnetic properties .....	14
1.3.3	Electromagnetic wave absorbing properties .....	16
<b>1.4</b>	<b>Conclusion</b>	<b>18</b>
<b>1.5</b>	<b>References</b>	<b>19</b>
<b>2</b>	<b>Application in Enhanced Oil Recovery</b> .....	<b>21</b>
<b>2.1</b>	<b>Introduction</b>	<b>21</b>
<b>2.2</b>	<b>Methodology</b>	<b>22</b>
<b>2.3</b>	<b>Results and discussion</b>	<b>22</b>
2.3.1	Sample XRD .....	22
2.3.2	Viscosity and IFT Test .....	23
<b>2.4</b>	<b>Conclusion</b>	<b>24</b>
<b>2.5</b>	<b>References</b>	<b>25</b>

<b>3</b>	<b>Electromagnetic Properties of Nanoparticles</b> .....	<b>27</b>
<b>3.1</b>	<b>Introduction</b>	<b>27</b>
<b>3.2</b>	<b>Material and methods</b>	<b>28</b>
<b>3.3</b>	<b>Results and discussion</b>	<b>28</b>
3.3.1	Powder X-ray diffraction of the as-prepared materials .....	28
3.3.2	Surface morphology study .....	29
3.3.3	Reflection and transmission coefficient .....	30
<b>3.4</b>	<b>Conclusion</b>	<b>30</b>
<b>3.5</b>	<b>References</b>	<b>31</b>
<b>4</b>	<b>Solar Electricity Generation</b> .....	<b>33</b>
<b>4.1</b>	<b>Introduction</b>	<b>33</b>
<b>4.2</b>	<b>Literature Review</b>	<b>35</b>
4.2.1	Problems in PV based electricity generation .....	35
4.2.2	Sun Tracking Systems .....	36
4.2.3	Data Acquisition System (DAS) .....	37
4.2.4	Diagnostic Mechanism .....	38
<b>4.3</b>	<b>Research Methodology</b>	<b>38</b>
4.3.1	Performance monitoring phase .....	38
4.3.2	Control Phase .....	39
4.3.3	Data Acquisition Board .....	39
4.3.4	Solar Irradiation Measurement .....	40
<b>4.4</b>	<b>Results and discussion</b>	<b>41</b>
4.4.1	Sun Tracking System .....	41
4.4.2	Data Acquisition Board .....	43
4.4.3	Diagnostic Mechanism .....	43
<b>4.5</b>	<b>Conclusion</b>	<b>44</b>
<b>4.6</b>	<b>References</b>	<b>45</b>
<b>5</b>	<b>Computerized Data Acquisition System</b> .....	<b>49</b>
<b>5.1</b>	<b>Introduction</b>	<b>49</b>
<b>5.2</b>	<b>Problem Formulation</b>	<b>50</b>
<b>5.3</b>	<b>Current Education System In Malaysia</b>	<b>50</b>
<b>5.4</b>	<b>Computerized Data Acquisition System</b>	<b>51</b>
<b>5.5</b>	<b>Critical Analysis</b>	<b>53</b>
<b>5.6</b>	<b>Research Objectives</b>	<b>53</b>
<b>5.7</b>	<b>Methodology</b>	<b>53</b>
5.7.1	Hardware Understanding and Implementation .....	53
5.7.2	Software Requirement and Implementation .....	53
<b>5.8</b>	<b>Results and discussion</b>	<b>56</b>
5.8.1	Experiment Testing .....	58
<b>5.9</b>	<b>Conclusion</b>	<b>59</b>
<b>5.10</b>	<b>References</b>	<b>59</b>

<b>6</b>	<b>Competitive Adsorption of Phenol and 4-CP</b> .....	<b>65</b>
<b>6.1</b>	<b>Introduction</b>	<b>65</b>
<b>6.2</b>	<b>Materials and Methods</b>	<b>67</b>
6.2.1	Materials .....	67
6.2.2	CCD design of experimental run .....	67
6.2.3	Set up procedure of adsorption study .....	67
<b>6.3</b>	<b>Results and discussion</b>	<b>68</b>
6.3.1	Competitive adsorption of phenol and 4-CP .....	68
6.3.2	Analysis of variance (ANOVA) of statistical models .....	69
6.3.3	Optimization of interactive factors .....	70
<b>6.4</b>	<b>Conclusion</b>	<b>70</b>
<b>6.5</b>	<b>References</b>	<b>73</b>
<b>7</b>	<b>Chemical Enhanced Oil Recovery (CEOR)</b> .....	<b>75</b>
<b>7.1</b>	<b>Introduction</b>	<b>75</b>
<b>7.2</b>	<b>Problem Statement</b>	<b>76</b>
<b>7.3</b>	<b>Literature Review</b>	<b>76</b>
7.3.1	Enhanced Oil Recovery (EOR) .....	76
7.3.2	Surfactants .....	77
<b>7.4</b>	<b>Ionic Liquids (ILs)</b>	<b>77</b>
<b>7.5</b>	<b>Methodology</b>	<b>78</b>
7.5.1	Synthesis of (HMIM)(DOSS) .....	78
7.5.2	Characterization of (HMIM)(DOSS) .....	79
7.5.3	IFT Using Hybrid Ionic Liquid .....	79
<b>7.6</b>	<b>Result and discussion</b>	<b>79</b>
7.6.1	Properties of Crude Oil .....	79
7.6.2	Water Content Analysis .....	80
7.6.3	NMR and Ion Chromatography .....	80
7.6.4	Thermogravimetry Analysis (TGA) .....	80
7.6.5	Interfacial Tension (IFT) Experiment .....	80
7.6.6	Cost Evaluation .....	84
<b>7.7</b>	<b>Conclusion</b>	<b>85</b>
<b>7.8</b>	<b>References</b>	<b>86</b>
<b>8</b>	<b>Ionic Liquid in Desulfurization Process</b> .....	<b>89</b>
<b>8.1</b>	<b>Application of 1-butyl-3-methylimidazolium dibutylphosphate for the extraction of benzothiophene from model oil</b>	<b>89</b>
<b>8.2</b>	<b>Introduction</b>	<b>89</b>
<b>8.3</b>	<b>Experimental</b>	<b>90</b>
8.3.1	Synthesis and characterization of (BMIM)(DBP) .....	90
8.3.2	Characterization of (BMIM)(DBP) .....	90
8.3.3	Liquid-liquid extraction of model crude .....	90

<b>8.4</b>	<b>Results and discussion</b>	<b>91</b>
8.4.1	Synthesis and Characterization of (BMIM)(DBP) .....	91
8.4.2	Liquid-liquid extraction .....	92
<b>8.5</b>	<b>Conclusion</b>	<b>93</b>
<b>8.6</b>	<b>References</b>	<b>94</b>
<b>9</b>	<b>Catalyst for Propane Ammoxidation .....</b>	<b>97</b>
<b>9.1</b>	<b>Introduction</b>	<b>97</b>
<b>9.2</b>	<b>Materials and Methods</b>	<b>98</b>
<b>9.3</b>	<b>Results and Discussion</b>	<b>99</b>
<b>9.4</b>	<b>Conclusion</b>	<b>101</b>
<b>9.5</b>	<b>References</b>	<b>102</b>

### III

## Mathematics

<b>10</b>	<b>Visible Light Communication System .....</b>	<b>105</b>
<b>10.1</b>	<b>Introduction</b>	<b>105</b>
<b>10.2</b>	<b>System configurations</b>	<b>106</b>
<b>10.3</b>	<b>Results and discussion</b>	<b>108</b>
10.3.1	Optical power distribution .....	108
10.3.2	RMS delay spread .....	109
10.3.3	Uplink bandwidth estimation .....	112
<b>10.4</b>	<b>Conclusion</b>	<b>112</b>
<b>10.5</b>	<b>References</b>	<b>113</b>
<b>11</b>	<b>Seismic Ray Tracing Method .....</b>	<b>115</b>
<b>11.1</b>	<b>Introduction</b>	<b>115</b>
<b>11.2</b>	<b>Methodology</b>	<b>116</b>
<b>11.3</b>	<b>Results and discussion</b>	<b>117</b>
<b>11.4</b>	<b>Conclusion</b>	<b>120</b>
<b>11.5</b>	<b>References</b>	<b>121</b>
<b>12</b>	<b>Global Positioning System (GPS) .....</b>	<b>123</b>
<b>12.1</b>	<b>Introduction</b>	<b>123</b>
<b>12.2</b>	<b>Tropospheric Delay</b>	<b>124</b>
<b>12.3</b>	<b>Mapping Function</b>	<b>124</b>
12.3.1	Mapping Function Model Description .....	124
12.3.2	Neill Mapping Function (NMF, 1996) .....	125
12.3.3	Simplification of hydrostatic Neill mapping function, NMF(h) .....	126
12.3.4	Sum of Error Calculation For hydrostatic Neill Mapping Function, NMF(h) ...	127
<b>12.4</b>	<b>Conclusion</b>	<b>128</b>
<b>12.5</b>	<b>References</b>	<b>129</b>

<b>13</b>	<b>External Power Source for RFID Tags</b> .....	<b>131</b>
<b>13.1</b>	<b>Introduction</b>	<b>131</b>
<b>13.2</b>	<b>Thermoelectric Generator (TEG) Module</b>	<b>133</b>
<b>13.3</b>	<b>Methodology</b>	<b>134</b>
13.3.1	Inductor Coil Transformer .....	134
13.3.2	Circuit Design .....	134
<b>13.4</b>	<b>Results and discussion</b>	<b>135</b>
<b>13.5</b>	<b>Conclusion</b>	<b>138</b>
<b>13.6</b>	<b>References</b>	<b>139</b>
<b>14</b>	<b>Biodegradation</b> .....	<b>141</b>
<b>14.1</b>	<b>Introduction</b>	<b>141</b>
<b>14.2</b>	<b>Mathematical Model</b>	<b>141</b>
<b>14.3</b>	<b>Results and discussion</b>	<b>143</b>
<b>14.4</b>	<b>Conclusion</b>	<b>143</b>
<b>14.5</b>	<b>References</b>	<b>144</b>



# Physics

<b>1</b>	<b>Ferrite-CNT-Polymer Composite</b> .....	<b>11</b>
1.1	Introduction	
1.2	Experimental	
1.3	Results and discussion	
1.4	Conclusion	
1.5	References	
<b>2</b>	<b>Application in Enhanced Oil Recovery</b>	<b>21</b>
2.1	Introduction	
2.2	Methodology	
2.3	Results and discussion	
2.4	Conclusion	
2.5	References	
<b>3</b>	<b>Electromagnetic Properties of Nanoparticles</b> .....	<b>27</b>
3.1	Introduction	
3.2	Material and methods	
3.3	Results and discussion	
3.4	Conclusion	
3.5	References	
<b>4</b>	<b>Solar Electricity Generation</b> .....	<b>33</b>
4.1	Introduction	
4.2	Literature Review	
4.3	Research Methodology	
4.4	Results and discussion	
4.5	Conclusion	
4.6	References	
<b>5</b>	<b>Computerized Data Acquisition System</b>	<b>49</b>
5.1	Introduction	
5.2	Problem Formulation	
5.3	Current Education System In Malaysia	
5.4	Computerized Data Acquisition System	
5.5	Critical Analysis	
5.6	Research Objectives	
5.7	Methodology	
5.8	Results and discussion	
5.9	Conclusion	
5.10	References	

## 12. Global Positioning System (GPS)

### NEILL'S MAPPING FUNCTION SIMPLIFICATION FOR DRY COMPONENT USING REGRESSION METHODS

The modeling of the GPS tropospheric delay mapping function should be revised by simplifying its mathematical model. The current tropospheric delay models use mapping functions in the form of continued fractions. This model is quite complex and need to be simplified. By using regression method, the dry (hydrostatics) mapping function models has been selected to be simplified. There are twenty six operations for dry mapping function component of Neill Mapping Function (NMF), to be carried out before getting the mapping function scale factor. So, there is a need to simplify the mapping function models to allow faster calculation and also better understanding of the models.

#### 12.1 Introduction

The issue of atmospheric delay of Global Positioning system (GPS) signal is now extensively investigated to minimize the positioning error due to atmospheric delay, especially tropospheric and ionospheric delay (Sakidin, 2012a). The refraction index is a function of the actual tropospheric path through which the ray passes. The ray's path begins at the receiver antenna ending at the last point of the effective troposphere. Tropospheric delay refers to the refraction of the GPS signal as it passes through the neutral atmosphere from the satellite to the earth. The effect causes the distance traveled by the signal to be longer than the actual geometric distance between the satellite and receiver. Hence, there is a need to introduce the simpler mathematical modeling of the mapping function model to increase the understanding of the model (Leick, 1995).

Many atmospheric models were established by using many approaches. However the difficulty in modeling the tropospheric effect, especially water vapor is the main reason why the researchers are still looking for better model for reducing the tropospheric error. Troposphere behaves like a non dispersive medium, whereby the refraction is independent of the frequency of the signals passing through it, so troposphere effect cannot be eliminated via dual-frequency observations (Leick, 1995).

## 12.2 Tropospheric Delay

The tropospheric delay is measured in distance, and a typical zenith tropospheric delay would be between 2.3m to 2.5m (Misra & Enge, 2001), meaning that the troposphere causes a GPS range observation to have an apparent additional 2.5m distance between the ground based receiver and a satellite at zenith. The delay caused by the troposphere can be separated into two main components such as the hydrostatic delay and the wet delay (Saastamoinen, 1972). The hydrostatic delay is caused by the dry part of gases in the atmosphere, while the wet delay is caused solely by highly varying water vapor in the atmosphere. The hydrostatic delay makes up approximately 90% of the total tropospheric delay. The hydrostatic delay is entirely dependent on the atmospheric weather characteristics found in the troposphere. The hydrostatic delay in the zenith direction is typically about 2.3m (Businger et al., 1996 & Dodson et al., 1996).

Tropospheric delay can be reduced by using smaller mapping function. As a coefficient to the zenith tropospheric delay for both dry and also wet components, the value of mapping function can affect the total tropospheric delay. Mapping function depends on the elevation angle and produce larger value of mapping function by decreasing the elevation angle, especially for the elevation angles less than 5 degree (Sakidin & Chuan, 2012b). There is a need to minimize the mapping function in order to improve the total tropospheric delay for GPS signal. Saastamoinen model (1972) is selected for tropospheric delay calculation due to its accuracy about 3cm in zenith and this model is widely used for high accuracy GPS positioning (Mendes, 1999).

## 12.3 Mapping Function

### 12.3.1 Mapping Function Model Description

The tropospheric delay is the shortest in zenith direction and will become larger with increasing zenith angle. Projection of zenith path delays into slant direction is performed by application of a mapping function or obliquity factor, is defined as (Schuler, 2001):

$$m(z) = \frac{SND}{ZND} = \frac{TD}{ZND} \quad (12.1)$$

where,

*SND*: slant neutral delay or total tropospheric delay (TD),

*ZND*: zenith neutral delay (total zenith delay). Referring to Figure 12.1, the tropospheric delay is shortest in zenith direction when the satellite at P and will become larger with increasing zenith angle at Q.

For neutral component,

$$\cos z = \frac{1}{m(z)} \quad (12.2)$$

Equation (12.2) can be written as:

$$m(z) = \frac{1}{\cos z} = \sec z \quad (12.3)$$

Unfortunately, this secant model is only an approximation assuming a planar surface of the earth and not taking the curvature of the earth into account. Moreover, the temperature and water vapor distribution may cause deviations from this simple formula. It can only be used for small zenith angle, from 0° to 60° (Saastamoinen, 1972). TD (total tropospheric delay) can be separated into two components such as a hydrostatic component (zenith hydrostatic delay, ZHD) and a wet component (zenith wet delay, ZWD) with their mapping function,  $m(z)$  as given below:

$$TD = (ZHD + ZWD)m(z) \quad (12.4)$$

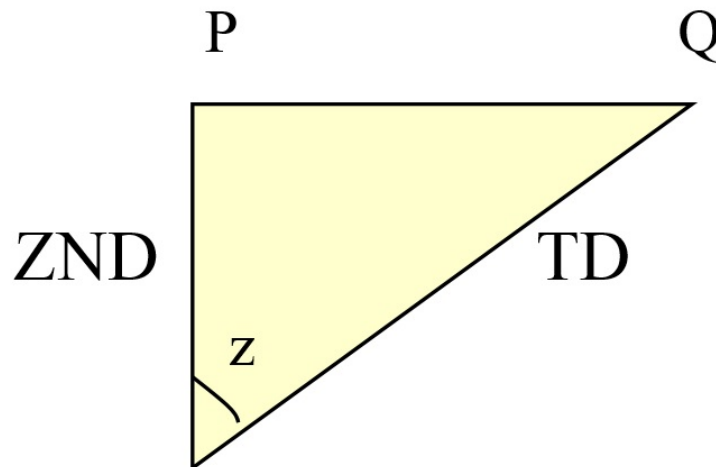


Figure 12.1: Obliquity factor (mapping function) between zenith and slant direction (Sakidin and Chuan, 2012c).

In some cases, the mapping functions for wet and hydrostatic components are different. This representation allows the use of separate mapping functions for the hydrostatic and wet delay components (Schuler, 2001):

$$TD = ZHDm_h(\epsilon) + ZWDm_w(\epsilon) \quad (12.5)$$

where, ZHD : zenith hydrostatic delay (m) ZWD : zenith wet delay (m)  $m_h(\epsilon)$ : the hydrostatic mapping function (no unit)  $m_w(\epsilon)$ : the wet mapping function (no unit)

Nowadays, many modern mapping functions such as *UNBabc*, *UNBab*, Neill and some others have been established in a form of continued fraction, which introduce many operations. The number of operations for those mapping function models should be reduced from continued fraction form into simpler form to allow shorter computing time and better understanding of the models, but at the same time can give similar value for the mapping function scale factor (Sakidin, Ahmad & Bugis, 2014a).

### 12.3.2 Neill Mapping Function (NMF, 1996)

Neill (1996) proposed the new mapping function (*NMF*) based on temporal changes and geographic location rather than on surface meteorological parameters. He argued that all previously available mapping functions have been limited in their accuracy by the dependence on surface temperature, which causes three dilemmas. All of these are because there is more variability in temperature in the atmospheric boundary layer, from the Earth's surface up to 2000 m. First, diurnal alterations in surface temperature cause much smaller variations than those calculated from the mapping functions. Second, seasonal changes in surface temperature are normally larger than upper atmosphere changes (but the computed mapping function yields artificially large seasonal variations). Third, the computed mapping function for cold summer days may not significantly differ from warm winter days. For example, actual mapping functions are quite different than computed values because of the difference in lapse rates and heights of the troposphere.

The new mapping functions have been derived from temperature and relative humidity profiles, which are in some sense averages over broadly varying geographical regions. Neill (1996) compared and ray traces calculated from radiosonde data spanning about one year or more covering a wide range of latitude and various heights above sea level. Such comparison was to ascertain the validity

and applicability of the mapping functions. Through the least-square fit of four different latitude data sets, Niell (1996) showed that the temporal variation of the hydrostatic mapping function is sinusoidal within the scatter of the data.

The mapping functions derived by Arthur Neill in 1996, are the most widely used, and are known to be the most accurate and easily-implemented functions (Ahn, 2005). Neill Mapping Function hydrostatics component given in equation (12.6) below,

$$m_h(\varepsilon) = \frac{1 + \frac{a_h}{1 + \frac{b_h}{1 + c_h}}}{\sin \varepsilon + \frac{a_h}{\sin \varepsilon + \frac{b_h}{\sin \varepsilon + c_h}}} + \left[ \frac{1}{\sin \varepsilon} - \left( \frac{1 + \frac{a_{ht}}{1 + \frac{b_{ht}}{1 + c_{ht}}}}{\sin \varepsilon + \frac{a_{ht}}{\sin \varepsilon + \frac{b_{ht}}{\sin \varepsilon + c_{ht}}}} \right) \right] H \quad (12.6)$$

where,  $\varepsilon$ : elevation angle  $m_h$ : hydrostatics mapping function  $H$ : station height above sea level (km).

For the hydrostatics *NMF* mapping function, the parameter  $a_h$  at tabular latitude  $\varphi_i$  at time  $t$  from January 0.0 (in UT days) is given as:

$$a_h(\varphi, t) = a_{avg}(\varphi) + a_{amp}(\varphi) \cos \left( \frac{t - DOY}{365.25} 2\pi \right) \quad (12.7)$$

where DOY (day of year) is the adopted phase, DOY = 28 for Northern hemisphere and DOY = 211 for Southern hemisphere. The linear interpolation between the nearest  $a_h(\varphi, t)$  is used to obtain the value of parameter  $a_h(\varphi, t)$  which is stated as parameter  $a_h$  in equation (12.6). For parameters  $b_h$  and  $c_h$ , the same procedure can be applied. Height correction coefficients are given as  $a_{ht}$ ,  $b_{ht}$  and  $c_{ht}$  were determined by a least-squares fit to the height correction at nine elevation angles (Neill, 1996).

Mendes (1999) analyzed the large number of mapping functions by comparing against radiosonde profiles from 50 stations distributed worldwide (32,467 benchmark values). The models that meet the high standards of modern space geodetic data analysis are Ifadis (1993), Lanyi (1984), Herring (1992), and Neill (1994). He found that for elevation angle above 15 degrees, the models Lanyi (1984), Herring (1992), and Neill (1994) yield identical mean biases and the best total error performance. At lower elevation angles, Ifadis (1993) and Neill (1994) are superior.

### 12.3.3 Simplification of hydrostatic Neill mapping function, NMF(h)

Regression method is used to find the same type of graph for the original NMF. However there is a slight difference for some points of the graph. From the statistical analysis, the difference between the original and the simplified model is small and not significant as described below.

NMF(h) model has been named as Y, while the simplified models have been named as Y1, Y2 and Y3. These four mapping function models give a graph of parabolic shape. However there is a slight difference between the Y model and the simplified models.

The simplified models (Y1, Y2 and Y3) have been generated using regression method, which give the model in a form of (Sakidin and Chuan, 2012b).

$$Y1 = AX^B \quad (12.8)$$

where Y1: simplified NMF(h),  $A, B$ : constant,  $X$ : elevation angle (independent variable).

This model is simpler than the original Y mapping function. By using these simplified models, we can reduce the computation time from 26 operations to only 2 operations. Model Y1 has been generated from regression method, whereby model Y2 and Y3 have been generated based on Y1 model. Model Y2 is formed by fixing the value of constant B and changing the value of constant A; while model Y3 is formed by fixing the value of constant A and changing the value of constant B. Model Y2 and Y3 are formed when they give unity when X is 90 degree.

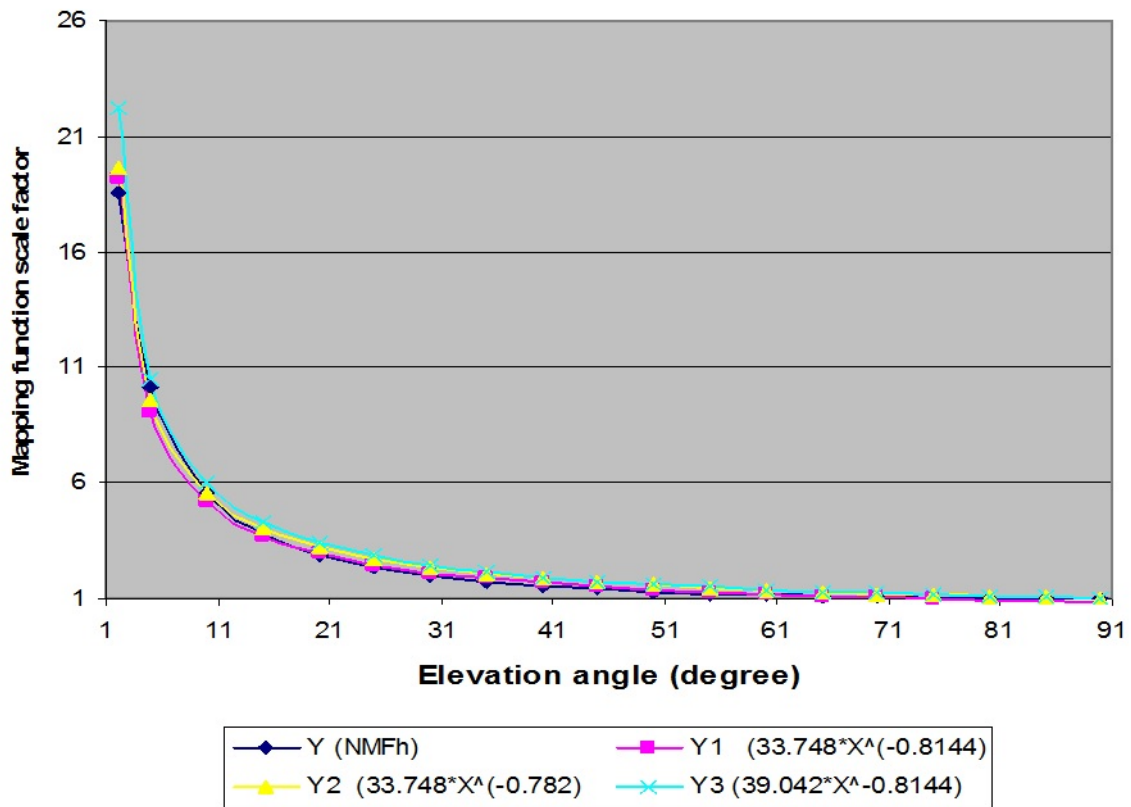


Figure 12.2: Graph of NMF(h) mapping function by regression.

### 12.3.4 Sum of Error Calculation For hydrostatic Neill Mapping Function, NMF(h)

Sum of error method can be used to show how the simplified models deviate from the original model. The smaller deviation is better, which shows that the simplified model is closer to the original model.

From the Table 3.1 above, although the sum of error is small (1.76), the Y1 model has not been selected due to it does not meet the constraint requirement (0.86), which is at 90 degree the mapping function scale factor should be unity. That is the constraint used in finding the mapping function model. Although the Y3 model meets the requirements, whereby the model gives big value of sum of error (14.21), which is most of the points are scattered quite far from the original NMF(h) mapping function model.

So,  $Y2 = 33.748X^{-0.782}$  model has been selected as the simplification mapping function model for NMF(h) due the smallest sum of error (1.94) compared to the others and it's mapping function gives unity at 90 degree elevation angle as given in Figure 12.2 below.

Table 12.1: Reduction percentage of model operation.

Model	Number of operations (Current method)	Number of operations (Regression method)	Reduction	%Reduction
NMF (h)	26	2	24	92.3

## 12.4 Conclusion

After the designed and developed prototype being tested by simulation and experiment respectively, it was found that the developed circuit can operate with low input voltage from TEG. Several improvements were made by changing the transistor type and the coil configuration in order to increase the efficiency of the circuit. The circuit was working well as expected when using 1:3 coil configuration. The bright blue LED lightened up and it showed us that the TEG module shall be used as power supply for low power consumption devices that consumed current of about 20mA and voltage of about 3V. In conclusion, use of TEG as source of power supply has vast potential to be explored as it has the potential to replace the current practice of using battery as source of supply. It is a free energy source as the electrical energy produces is being harvested from heat of human body and this shall reduce the cost as expected.

## 12.5 References

- [1] Landt, J. (2005). The History of RFID. *Potentials IEEE*, 24(4), 8-11.
- [2] Hosaka, R. (2007). An analysis for specifications of medical use RFID system as a wireless communication. *Engineering in Medicine and Biology Society*, 2007. EMBS 2007, 29th Annual International Conference of the IEEE, vol., no., pp. 2795-2798.
- [3] Meng, Q., Jin, J. (2011). Design of low power active RFID tag in UHF band. *Control, Automation and Systems Engineering (CASE)*, pp.1-4, pp. 30-31.
- [4] Nakao, S., Norimatsu, T., Yamazoe, T., Oshima, T., Watanabe, K., Minatozaki, K., Kobayashi, K. (2011). UHF RFID mobile reader for passive and active-tag communication, radio and wireless symposium (RWS). *IEEE Conferences*, 311-314.
- [5] V. Daniel Hunt, Albert Puglia, Mike Puglia. 2007. *A Guide to Radio Frequency Identification*, USA. Wiley Publication.
- [6] Harold G. Clampitt. 3rd edition 2007. *The RFID Certification*. Wiley Publication.
- [7] Steven Shepard. 2005. *Radio Frequency Identification*. USA. McGraw Hill Publication.
- [8] Dennis E. Brown. (2007). *RFID Implementation*, USA. Mc Graw Hill Publication.
- [9] Bhattacharya, M., Chu, C.H., Mullen, T. (2008). A Comparative Analysis of RFID Adoption in Retail and Manufacturing Sectors. *IEEE International Conference*, 241-249.
- [10] Watanabe, S. (2001). Wrist watch having thermoelectric generator (U.S 6304520 B1)
- [11] Jeffrey, G., Caillat, T. (2003). Using the compatibility factor to design high efficiency segmented thermoelectric generators. *MRS Proceedings*, 793, S2.1.
- [12] Jones, A., Hoare, R., Dontharaju, S., Tung, S., Sprang, R., Fazekas, J., Chain, J., Mickle, M. (2007). An automated, FPGA-based reconfigurable, low-power RFID tag. *Microprocessors and Microsystems*, 116-134.
- [13] Tiliute, D. E. (2007). Battery management in wireless sensor networks. *Electronics and Electrical Engineering*, Kaunas Technology, 9-12.
- [14] Damaschke, J. M. Design of a low input voltage converter for thermoelectric generator. *IEEE Transaction on Industry Applications*, 1203-1207.
- [15] Agawa, K., Aliotp, M., Zhou, W., Liu, T.T., Alarcon, L., Hajkazemshirazi, K., John, M., Richmond, J., Li, W., Rabaey, J. (2010). Design and verification of an ultra low power active RFID tag with multiple power domains. *Proc SASIMI*, 386-394.

### Authors

Hamzah Sakidin

Department of Fundamental and Applied Sciences,  
Universiti Teknologi PETRONAS,  
32610 Bandar Seri Iskandar, Perak

Siti Rahimah Batcha

Department of Fundamental and Applied Sciences,  
Universiti Teknologi PETRONAS,  
32610 Bandar Seri Iskandar, Perak

Asmala Ahmad

Faculty of Information Technology and Communication,  
Universiti Teknikal Malaysia Melaka  
76100 Durian Tunggal Melaka

Table 12.2: Sum of error for NMF(h), Y and simplified models (Y1, Y2, Y3).

X	$Y = NMF(h)$	$Y_1 = 33.748X^{-0.8144}$	$Y_2 = 33.748X^{-0.782}$	$Y_3 = 39.042X^{-0.8144}$	$Y - Y_1)^2$	$(Y - Y_2)^2$	$(Y - Y_3)^2$
2	18.58	19.19	19.63	22.20	0.37	1.09	13.10
5	10.15	9.10	9.59	10.53	1.11	0.32	0.14
10	5.56	5.17	5.58	5.99	0.15	0.00	0.16
20	2.89	2.94	3.24	3.40	0.00	0.12	0.26
30	1.99	2.12	2.3	2.45	0.02	0.14	0.21
40	1.55	1.67	1.89	1.94	0.01	0.11	0.15
50	1.30	1.39	1.58	1.61	0.01	0.08	0.09
60	1.15	1.20	1.37	1.39	0.00	0.05	0.06
70	1.06	1.06	1.22	1.23	0.00	0.02	0.03
80	1.02	0.95	1.09	1.10	0.00	0.01	0.01
90	1.00	0.86	1.00	1.00	0.09	0.00	0.00
Sum of Error					1.76	1.94	14.21